Accepted for publication in the proceedings of IEEE ICC 2023, Rome, Italy, 28 May - 01 June 2023

Short-Packet Communication Assisted Reliable Control of UAV for Optimum Coverage Range

Sourabh Solanki*, Vibhum Singh*, Sumit Gautam†,*, Jorge Querol*, and Symeon Chatzinotas*

*Interdisciplinary Centre for Security, Reliability and Trust (SnT), University of Luxembourg, Luxembourg
†Department of Electrical Engineering, Indian Institute of Technology Indore, India

Email:{sourabh.solanki, vibhum.singh, jorge.querol, symeon.chatzinotas}@uni.lu, sumit.gautam@iiti.ac.in

***Abstract*—The reliability of command and control (C2) operation of the UAV is one of the crucial aspects for the success of UAV applications beyond 5G wireless networks. In this paper, we focus on the short-packet communication to maximize the coverage range of reliable UAV control. We quantify the reliability performance of the C2 transmission from a multi-antenna ground control station (GCS), which also leverages maximal-ratio transmission beamforming, by deriving the closed-form expression for the average block error rate (BLER). To obtain additional insights, we also derive the asymptotic expression of the average BLER in the high-transmit power regime and subsequently analyze the possible UAV configuration space to find the optimum altitude. Based on the derived average BLER, we formulate a joint optimization problem to maximize the range up to which a UAV can be reliably controlled from a GCS. The solution to this problem leads to the optimal resource allocation parameters including blocklength and transmit power while exploiting the vertical degrees of freedom for UAV placement. Finally, we present numerical and simulation results to corroborate the analysis and to provide various useful design insights.**

I. Introduction

UAVs are envisioned to play a pivotal role in the development of non-terrestrial networks beyond 5G [1]. For the successful deployment of UAV-based wireless networks, ensuring air-space regulatory compliance and other safety measures are of paramount importance. Various countries establish their own set of requirements for using the air-space. For instance, NASA in the United States is responsible for the specific guidelines for UAV traffic management. Similarly, in Europe, the U-space program under the SESAR joint undertaking aims to establish the requirements for UAVs in European airspace [2]. In this vein, the reliability of the control and non-payload communication (CNPC), also known as command and control (C2), to UAV is critical to satisfy the strict guidelines. In addition, the latency to control the UAV should be as low as possible to avoid a delay in the real-time navigation of the UAV.

Ultra-reliable and low-latency communication (URLLC) services for C2 of UAVs are potentially useful for safe flight operations and emergency situations. As such, short-packet or finite blocklength transmission is considered to be an enabler of the URLLC at the physical layer level [3]. In fact, various works have studied the different aspects of UAV networks considering short-packet communication [4]–[9]. For instance, the authors studied a joint blocklength and location optimization problem in [4] and joint transmit power and placement optimization [5] for UAV relay systems. In [6], the achievable data rate was analyzed considering a 3D channel model. Further, packet error probability and effective throughput are derived in [7] for URLLC-based UAV communications. However, all these works did not incorporate the effect of small scale fading which is dominated in the dense-urban environment. In contrast, by incorporating small- and large-scale fading, the authors in [8] analyzed the reliability performance of full-duplex multi-UAV networks, while the work in [9] studied a cooperatively relaying UAV to investigate the optimal blocklength and power in the UAV.

As noted above, the reliability of C2 communication for UAVs is critical to the success of UAV applications. To this end, differently from existing studies, this paper focuses on URLLC-assisted UAV to maximize the range of reliable UAV control. Specifically, our contributions can be summarized as follows:

- We quantify the reliability performance of the short-packet communication-assisted UAV control from a multi-antenna ground station, which also performs maximal-ratio transmission (MRT) beamforming, by deriving the closed-form expression for the average block error rate (BLER).
- To obtain additional insights, we also derive the asymptotic expression for the average BLER in the high-transmit power regime and subsequently obtain the UAV configuration space towards finding the optimum altitude.
- Moreover, we formulate a joint optimization problem to find the maximum coverage up to which a UAV can be reliably controlled. Consequently, leveraging the vertical degrees of freedom for UAV placement, we obtain the optimal resource allocation parameters including blocklength and transmit power.

It is important to note that the study in this paper is useful for various emerging applications of UAV such as disaster resilient or emergency network services, hot-spot, on-demand aerial access point, etc. For such applications, reliable control of UAVs is very important to ensure safety compliance and other regulation guidelines.

Notations: Throughout this paper, we use $\mathbb{E}[\cdot]$ to represent the expectation and $\mathcal{CN}(0,\sigma^2)$ to represent the complex normal distribution having mean zero and variance σ^2. Also, $(\cdot)^T, (\cdot)^*, |\cdot|$, and $||\cdot||$ denote transpose, conjugate, absolute value, and Euclidean norm operations, respectively. $f_X(\cdot)$ and $F_X(\cdot)$ denote the probability density function (PDF) and the cumulative distribution function (CDF) of a random variable (RV) X, respectively, and $\mathbb{P}(\cdot)$ represents the probability.

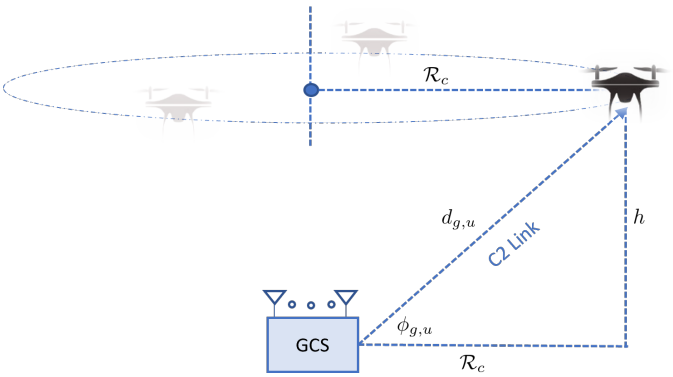

Fig. 1: System model

$Q^{-1}(\cdot)$ is inverse of the Gaussian Q-function such that $Q(x) = \int_x^\infty 1/\sqrt{2\pi}\exp(-t^2/2)dt$. $\Upsilon[\cdot,\cdot]$ and $\Gamma[\cdot]$ denote, respectively, the lower incomplete and the complete gamma functions [10].

II. System Descriptions

We consider C2 operation of a UAV from a GCS as shown in Fig. 1. The GCS is considered to be equipped with N_t number of antennas while UAV has a single antenna. In general, C2 for UAVs often requires low data rates. Also, safe navigation and regulatory compliance make UAV control a time-sensitive process. For URLLC applications, short-packet communication can be used for low-latency transmission [4]. Therefore, for efficient UAV control, we consider the short-packet communication link for the C2 between the UAV and the GCS [11]. Let h denotes the flying altitude of UAV and $\mathcal{R}_c$ indicates the coverage range for UAV control. Further, as can be seen from Fig. 1, the UAV follows a circular trajectory with radius $\mathcal{R}_c$. The GCS is located at the centre of the circular trajectory projected on the ground.

To model ground-to-air (G2A) propagation, we adopt a suitable channel model that accounts for both large-scale fading and small-scale fading. More specifically, the large-scale fading is primarily dependent on altitude, distance, and elevation angle, which are dominant factors for G2A propagation. As such, the line-of-sight (LoS) probability between the GCS and the UAV is given by [12], [13]

$$\mathbb{P}(\phi_{g,u}) = \frac{1}{1 + C\exp\left(-B(\phi_{g,u} - C)\right)}, \tag{1}$$

where $\phi_{g,u}$ represents the elevation angle between the GCS and the UAV, B and C are constants that depend on the environment, i.e., urban, dense urban, suburban, etc. Here, the height of the GCS is considered negligible compared with UAV altitude. Furthermore, based on the above formulations, the path-loss exponent is given by [13], [14]

$$\alpha(\phi_{g,u}) = \mathbb{P}(\phi_{g,u})c_g + f_g, \tag{2}$$

where c_g and f_g are constants. To characterize the small-scale fading, all the channel coefficients are subject to independent block Nakagami-m fading. In particular, let the channel $\boldsymbol{h_{g,u}}$ from GCS to UAV be a $N_t \times 1$ vector whose entries follow Nakagami-m distribution with fading severity parameter $m_{g,u}$ and average fading power $\Omega_{u,m}$. Nakagami-m distribution is a generalized model that can capture a variety of fading scenarios including Rician fading with parameter $m_{g,u} = \left(1 - \left(\frac{K}{k+1}\right)^2\right)^{-1}$ [15], with K being a Rician factor.

Let x_c represents the unit energy control signal, i.e., $\mathbb{E}[|x_c^2|] = 1$, transmitted from the GCS. The corresponding signal received at UAV is given by

$$y_u = \sqrt{P_g d_{g,u}^{-\alpha(\phi_{g,u})}}\boldsymbol{h}_{g,u}^T \boldsymbol{w} x_c + \eta_u, \tag{3}$$

where $d_{g,u} = \sqrt{(h^2 + \mathcal{R}_c^2)}$ is the distance between GCS and UAV, P_g is the transmit power, and $\eta_u \sim \mathcal{CN}(0, \sigma_o^2)$ denotes the additive white Gaussian noise (AWGN). The transmitter leverages MRT beamforming [16] such that the transmit beamforming vector $\boldsymbol{w} = \frac{\boldsymbol{h}_{g,u}^*}{||\boldsymbol{h}_{g,u}||}$. Based on (3), the instantaneous signal-to-noise ratio (SNR) at UAV to decode the control signal from GCS can be expressed as

$$\Lambda_{g,u} = \frac{P_g||\boldsymbol{h}_{g,u}^T\boldsymbol{w}||^2}{\sigma_o^2 d_{g,u}^{\alpha(\phi_{g,u})}} = \frac{P_g||\boldsymbol{h}_{g,u}||^2}{\sigma_o^2 d_{g,u}^{\alpha(\phi_{g,u})}}. \tag{4}$$

In (4), $||\boldsymbol{h}_{g,u}||^2$ can be characterized by the Gamma distribution whose PDF and CDF can be, respectively, given by

$$f_{||\boldsymbol{h}_{g,u}||^2}(x) = \left(\frac{m_{g,u}}{\Omega_{g,u}}\right)^{m_{g,u}N_t} \frac{x^{m_{g,u}N_t - 1}}{\Gamma(m_{g,u}N_t)} \exp\left(-\frac{m_{g,u}}{\Omega_{g,u}}x\right), \tag{5}$$

$$F_{||\boldsymbol{h}_{g,u}||^2}(x) = \frac{1}{\Gamma(m_{g,u}N_t)}\Upsilon\left(m_{g,u}N_t, \frac{m_{g,u}}{\Omega_{g,u}}x\right). \tag{6}$$

Recalling that GCS uses short-packet communication for sending the C2 information to UAV. Since the metadata becomes comparable to the payload data for the short-packet transmission, the classical Shannon's capacity theorem, which is valid for infinite blocklength, does not hold in this case. The achievable rate $R_{g,u}$ under a finite blocklength of N_p with a BLER $\Xi_{g,u}$ can be given by [16], [17]

$$R_{g,u} \approx \log_2(1 + \Lambda_{g,u}) - \sqrt{\frac{V_{g,u}}{N_p}}Q^{-1}(\Xi_{g,u}), \tag{7}$$

where $V_{g,u}$ is the channel dispersion and is given by

$$V_{g,u} = \left(1 - (1 + \Lambda_{g,u})^{-2}\right)(\log_2 e)^2. \tag{8}$$

The approximation in (7) is very accurate for $N_p \geq 100$. For an n_b number of data bits in the blocklength of N_p, the achievable rate can be given by $R_{g,u} = n_b/N_p$.

On the basis of the preceding formulation, in the next section, we investigate the BLER to measure the reliability performance of the control signal transmission.

III. Reliability Analysis

UAV's safe navigation is critical for its potential use cases in beyond 5G networks. Hence, the reliability of UAV's control is an important performance metric. We derive the BLER for UAV to analyze the reliability performance of control signal transmission from GCS. Firstly, rearranging (7), we can express the instantaneous BLER as

$$\Xi_{g,u} = Q\left(\sqrt{\frac{N_p}{V_{g,u}}}\left(\log_2(1 + \Lambda_{g,u}) - R_{g,u}\right)\right). \tag{9}$$

Using (9), the average BLER can be obtained as

$$\Xi_{g,u}^{\text{avg}} = \int_0^\infty \Xi_{g,u} f_{\Lambda_{g,u}}(x)dx, \tag{10}$$

where $f_{\Lambda_{g,u}}(\cdot)$ is the PDF of SNR $\Lambda_{g,u}$. Since it is difficult to derive the exact closed-form solution of (10), we adopt the following approximation [16] to first reduce (9) to

$$\Xi_{g,u} \approx \begin{cases} 1, & \Lambda_{g,u} \leq \xi_{g,u} \\ \frac{1}{2} - \vartheta\sqrt{N_p}(\Lambda_{g,u} - \varphi), & \xi_{g,u} < \Lambda_{g,u} < \delta_{g,u} \\ 0, & \Lambda_{g,u} \geq \delta_{g,u} \end{cases} \tag{11}$$

where $\varphi = 2^{2n_b/N_p} - 1$, $\vartheta = \frac{1}{2\pi\sqrt{\varphi}}$, $\xi_{g,u} = \varphi - \frac{1}{2\vartheta\sqrt{N_p}}$, $\delta_{g,u} = \varphi + \frac{1}{2\vartheta\sqrt{N_p}}$. Based on the above, the following theorem provides the closed-form expression for the average BLER at UAV for the integer values of fading severity parameter $m_{g,u}$.

Theorem 1: For the transmission of C2 signals from a GCS to a UAV, the average BLER as a function of $\mathcal{R}_c$ and h can be given by

$$\begin{aligned}\Xi_{g,u}^{\text{avg}}(\mathcal{R}_c, h) = 1 - \vartheta\sqrt{N_p} \sum_{l=0}^{m_{g,u}N_t-1} \frac{1}{l!} \frac{\Omega_{gu}P_g}{m_{g,u}\sigma_o^2} d_{g,u}^{-\alpha(\phi_{g,u})} \\ \times \left[\Upsilon\left(l+1, \frac{m_{g,u}\sigma_o^2}{\Omega_{gu}P_g} d_{g,u}^{\alpha(\phi_{g,u})} \delta_{g,u}\right) \right. \\ \left. - \Upsilon\left(l+1, \frac{m_{g,u}\sigma_o^2}{\Omega_{gu}P_g} d_{g,u}^{\alpha(\phi_{g,u})} \xi_{g,u}\right) \right].\end{aligned} \tag{12}$$

Proof: Refer to Appendix A. ∎

For the non-integer values of $m_{g,u}$, the BLER expression is given in the following corollary.

Corollary 1: For the non-integer values of $m_{g,u}$, the average BLER can be obtained as

$$\begin{aligned}\Xi_{g,u}^{\text{avg}}(\mathcal{R}_c, h) = \vartheta\sqrt{N_p} \sum_{l=0}^{M} \frac{1}{\Gamma(m_{g,u}+l+1)} \frac{\Omega_{gu}P_g}{m_{g,u}\sigma_o^2} d_{g,u}^{-\alpha(\phi_{g,u})} \\ \times \left[\Upsilon\left(m_{g,u}+l+1, \frac{m_{g,u}\sigma_o^2}{\Omega_{gu}P_g} d_{g,u}^{\alpha(\phi_{g,u})} \delta_{g,u}\right) \right. \\ \left. - \Upsilon\left(m_{g,u}+l+1, \frac{m_{g,u}\sigma_o^2}{\Omega_{gu}P_g} d_{g,u}^{\alpha(\phi_{g,u})} \xi_{g,u}\right) \right].\end{aligned} \tag{13}$$

Proof: Refer to Appendix B. ∎

To simplify the derived BLER expression and get more insights, in the following corollary, we present its asymptotic approximation in the high transmit power regime, that is, $P_g \to \infty$.

Corollary 2: In the high-transmit power regime, the asymptotic expression of BLER can be obtained as

$$\begin{aligned}\Xi_{g,u}^{\text{asy}}(\mathcal{R}_c, h) \underset{P_g \to \infty}{\simeq} \frac{\vartheta\sqrt{N_p}}{\Gamma(m_{g,u}N_t+2)} \left(\frac{m_{g,u}\sigma_o^2}{\Omega_{gu}P_g} d_{g,u}^{\alpha(\phi_{g,u})}\right)^{m_{g,u}N_t} \\ \times \left(\delta_{g,u}^{m_{g,u}N_t+1} - \xi_{g,u}^{m_{g,u}N_t+1}\right).\end{aligned} \tag{14}$$

Proof: Refer to Appendix C. ∎

Remark 1: *It can be inferred from* (14) *that the BLER decreases with a shorter coverage radius, therefore, to achieve a smaller BLER, the coverage radius must be reduced. For practical applications, however, it is desirable to have a maximum possible coverage range for the UAV control in order to avoid frequent handovers. Therefore, there exists a trade-off between the coverage radius and the BLER. Nevertheless, a certain threshold of BLER can also ensure sufficient reliability of control signal transmission. To this end, the coverage radius can be maximized while satisfying a certain BLER, i.e., a target reliability, requirement necessary for guaranteeing the reliability.*

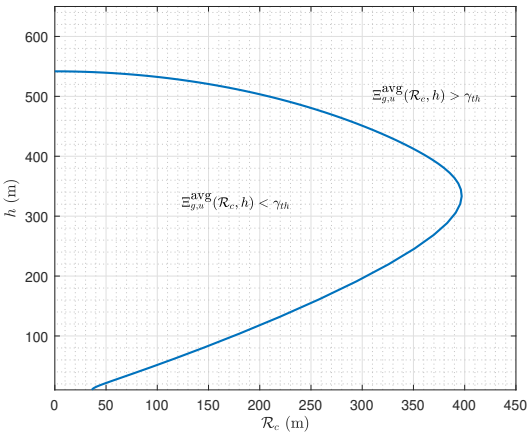

Fig. 2: Configuration space of UAV for a target BLER threshold

Remark 2: *Using the asymptotic expression in Corollary 2, we can determine the UAV configuration space which encompasses all possible* $(\mathcal{R}_c, h)$ *values for a given BLER. Concretely, we first re-express* (14) *to obtain*

$$d_{g,u} = \left(\frac{\Xi_{g,u}^{\text{asy}}(\mathcal{R}_c, h)}{\mathcal{B}}\right)^{\frac{1}{m_{g,u}N_t\alpha(\phi_{g,u})}}, \tag{15}$$

with

$$\begin{aligned}\mathcal{B} = \frac{\vartheta\sqrt{N_p}}{\Gamma(m_{g,u}N_t+2)} \left(\frac{m_{g,u}\sigma_o^2}{\Omega_{gu}P_g}\right)^{m_{g,u}N_t} \\ \times \left(\delta_{g,u}^{m_{g,u}N_t+1} - \xi_{g,u}^{m_{g,u}N_t+1}\right).\end{aligned} \tag{16}$$

Based on the (15)*, we can derive the following relation*

$$\mathcal{R}_c = d_{g,u} \cdot \cos(\phi_{g,u}), \tag{17a}$$

$$h = d_{g,u} \cdot \sin(\phi_{g,u}), \tag{17b}$$

with $\phi_{g,u} \in [0, \pi/2]$*. Using* (17)*, two-dimensional (2D) curve of the configuration space is demonstrated on a* $\mathcal{R}_c - h$ *plane in Fig. 2. Apparently, the maximum coverage is obtained corresponding to an optimal altitude on the boundary of the configuration space.*

IV. UAV Control Range Maximization

In this section, we formulate the problem to maximize the coverage for UAV's reliable control. The primary objective here is to maximize the coverage for UAV control while ensuring certain reliability requirement. Towards this goal, the

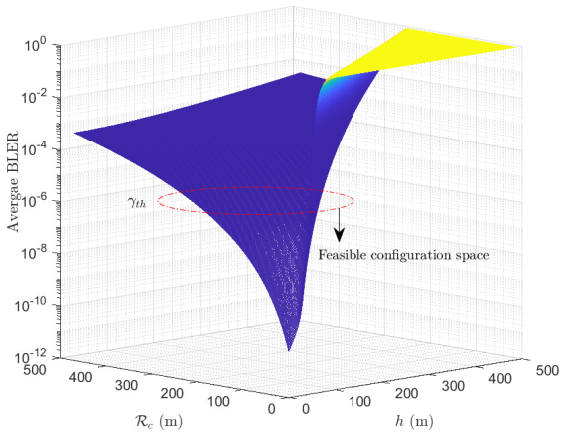

Fig. 3: Average BLER vs. altitude and coverage

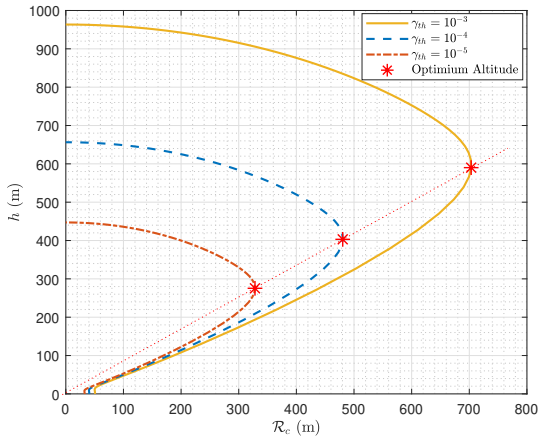

Fig. 4: Coverage vs. altitude of UAV

joint coverage maximization problem can be formulated as follows

$$(\mathbf{P}): \max_{h,P_g,N_p} \mathcal{R}_c,$$
$$\text{subject to}: \Xi_{g,u}^{\text{avg}}(\mathcal{R}_c, h) \leq \gamma_{th} \quad (18a)$$
$$0 \leq h \leq h_{\max} \quad (18b)$$
$$0 \leq P_g \leq P_{\max} \quad (18c)$$
$$0 \leq N_p \leq N_{p,\max} \quad (18d)$$

In the above formulation, constraint (18a) ensures the target reliability requirement necessary for UAV control. The feasible configuration space corresponding to this constraint can also be seen from a 3D curve in Fig. 3. Moreover, following the reasoning in **Remark 2**, the optimum coverage is obtained when equality in constraint (18a) holds. The limit in (18b), where $h_{\max}$ represents the maximum altitude of the UAV, restricts the altitude of the UAV to comply with the aviation authority requirements. The constraint in (18c) limits the maximum power at GCS. Intuitively, for maximizing the coverage, the GCS must transmit with the maximum available power and hence the equality in (18c) also holds such that $P_g^* = P_{\max}$. The blocklength is upper bounded by the constraint in (18d) which also translates to the latency constraint. Using (9), it can be seen that BLER decreases with increasing blocklength for a fixed data size as the Q-function is a monotonically decreasing function. Consequently, the best coverage is obtained at the maximum blocklength, that is, $N_p^* = N_{p,\max}$. As a result, problem (**P**) can be reduced to

$$(\mathbf{P1}): \max_{h} \mathcal{R}_c,$$
$$\text{subject to}: (18a), (18b).$$

To proceed further, we obtain the Lagrange dual function of the problem (**P1**) as

$$\mathcal{G}(\mathbf{\Lambda}) = \sup \mathcal{L}(\mathcal{R}_c, h, \lambda_i), \quad (20)$$

where the Lagrangian is given by

$$\mathcal{L}(\mathcal{R}_c, h, \lambda_i) = \mathcal{R}_c + \lambda_1 \left(\Xi_{g,u}^{\text{avg}}(\mathcal{R}_c, h) - \gamma_{th}\right) + \lambda_2(h - h_{\max}), \quad (21)$$

with $\mathbf{\Lambda} = (\lambda_1, \lambda_2)$ representing nonnegative dual variables associated with constraints (18a) and (18b). Thus, the resulting dual optimization problem becomes

$$(\mathbf{P2}): \min_{\mathbf{\Lambda}} \mathcal{G}(\mathbf{\Lambda}),$$
$$\text{subject to}: \mathbf{\Lambda} \geq 0.$$

It is a known fact that dual function is always convex by definition, and hence (**P2**) can be solved directly via standard convex optimization solvers [18]. Since we have obtained the closed-form expression of the average BLER, the evaluation of the optimal solution turns out to be quite efficient and fast. In addition, the optimal altitude can also be obtained by an exhaustive two-dimensional search within the feasible search space.

V. Numerical Results

This section analyzes the performance of the derived framework using the numerical and simulation results. For this, various parameters are set, unless otherwise stated, as follows [12], [16]: $\mathcal{C} = 0.5, \mathcal{B} = 20, e_u = -1.5, f_u = 3.5, m_{g,u} = 1, \Omega_{g,u} = 1, N_t = 3, h_{\max} = 1000$ m, $n_b = 80, N_{p,\max} = 100$, $P_{\max} = 30$ dBm, $\sigma_o^2 = -50$ dBm. The accuracy of the derived analytical results are also verified with extensive Monte Carlo simulations.

In Fig. 4, we plot the coverage range of UAV control against the altitude for different values of target reliability. Apparently, the lower the target reliability, higher will be the UAV control range. For example, the maximum range $\mathcal{R}_{c,\max} \approx 330$ m at $\gamma_{th} = 10^{-5}$ while $\mathcal{R}_{c,\max} \approx 703$ m at $\gamma_{th} = 10^{-3}$. Interestingly, the optimal altitude (h^*) corresponding to the maximum range ($\mathcal{R}_{c,\max}$) for various reliability targets lies along the same line. In other words, the ratio $h^*/\mathcal{R}_{c,\max}$ or the optimal elevation angle remains the same for different values of γ_{th}.

Fig. 5 demonstrates the effect of varying transmit power at GCS on the average BLER performance. For this, the coverage range is kept fixed at $\mathcal{R}_c = 300$ m, while the curves are plotted for two different values of the UAV altitudes. Evidently, the simulation results, denoted by markers, match with the analytical results, represented by solid lines, thus

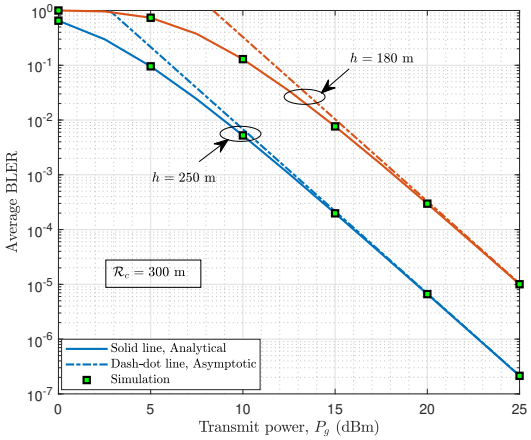

Fig. 5: Average BLER vs. transmit power

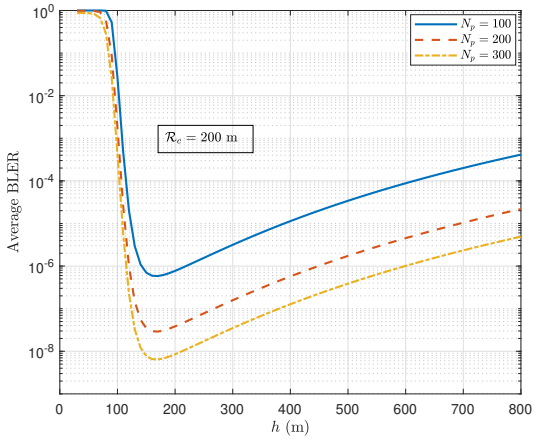

Fig. 6: Average BLER vs. altitude of UAV

verifying the accuracy of the theoretical analysis. In addition, the asymptotic curves are well aligned with the analytical and simulation results at the high-transmit power regime, confirming their accuracy. From the pertinent curves, it can be seen that the average BLER decreases with increasing transmit power, which is expected since higher transmit power leads to better received SNR at the UAV. This observation suggests that the range of UAV control can also be increased by increasing the transmit power, however, the constraint on the maximum transmit power at GCS inhibits the reduction in BLER after a certain point.

In Fig. 6, we illustrate the impact of blocklength on BLER performance. Clearly, a large blocklength leads to better average BLER performance. Interestingly, the minimum BLER is experienced at the same UAV altitude for different blocklength sizes. In other words, the optimal height remains unaffected of blocklength for a given coverage range. However, since a larger blocklength results in a smaller BLER, the coverage range can be increased for a given target reliability threshold. To exemplify this, for a target reliability of $\gamma_{th} = 10^{-5}$ (which corresponds to 99.999% reliability), the maximum coverage range is $\mathcal{R}_c \approx 330$ m for a blocklength of $N_p = 100$ while the maximum coverage range is $\mathcal{R}_c \approx 543$ m for a blocklength of $N_p = 200$. Nevertheless, larger blocklength translates to higher latency and thus it should be constrained to achieve low latency transmissions.

A. Impact of Aerial Interference

Although it would be desirable to have the dedicated resource blocks for the UAV C2 operations due to safety concerns, for the completeness, we analyze the effect of the interference from the neighbouring aerial vehicles on the maximum coverage range. For this, we consider air-to-air links to be modeled by a free space path loss model. Consequently, following (4), the signal-to-interference-plus-noise-ratio (SINR) at a UAV is given by $\Lambda_{g,u} = \frac{P_g ||\boldsymbol{h}_{g,u}||^2 d_{g,u}^{-\alpha(\phi_{g,u})}}{\sum_{i=1}^{L} P_i d_{i,u}^{-\alpha_o} + \sigma_o^2}$, where L is number of interferer, P_i is the transmit power at each interferers, $d_{i,u}$ is the distance between an i-th interferer and UAV, and α_o is the path-loss exponent. Using this SINR, the BLER can be derived following the similar approach as in Appendix A and hence its expression is omitted here for brevity. Analytical results are plotted in Fig. 7, while setting $P_i = 5$ dBm, $d_{i,u} = 300$ m, and $\alpha_o = 2$, for varying numbers of interferers and transmit antennas at GCS. Naturally, the presence of interference leads to a higher average BLER which, in turn, results in a relatively smaller coverage range. However, the loss in BLER performance can be compensated to some degree by increasing the number of antennas at GCS.

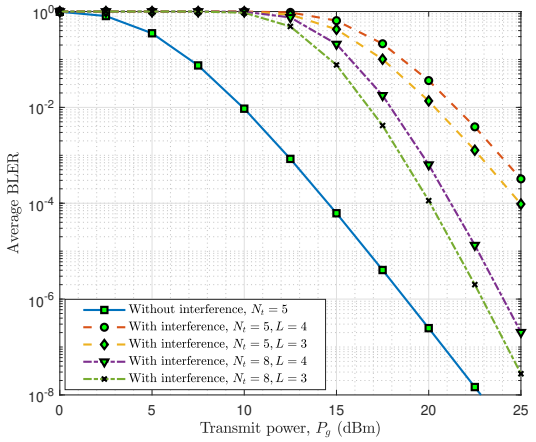

Fig. 7: Impact of aerial interference

VI. Conclusion

We studied a coverage range maximization problem for reliable UAV control. For URLLC-assisted C2 operation, we considered short-packet communication for control links between a multi-antenna ground control station and a UAV. Subsequently, we analyzed the reliability performance by deriving the closed-form expression for the average BLER. Further insights were obtained by delving into the asymptotic analysis at high transmit power regime. Finally, a joint optimization problem is solved to obtain the maximum coverage range upto which a UAV can be reliably controlled while optimally allocating the available resources leveraging the vertical degrees of freedom for UAV placement.

In essence, the developed framework leads to identification of a feasible flying space within which the UAV can be controlled reliably for various emerging applications.

Appendix A
Proof of Theorem 1

On invoking (11) in (10), we can re-express

$$\Xi_{g,u}^{\text{avg}} = \vartheta\sqrt{N_p}\int_{\xi_{g,u}}^{\delta_{g,u}} F_{\Lambda_{g,u}}(x)dx. \tag{A.1}$$

Using the SNR $\Lambda_{g,u}$ from (4), the CDF $F_{\Lambda_{g,u}}(x)$, with the aid of (6), can be derived as

$$F_{\Lambda_{g,u}}(x) = \Pr\left[\frac{P_g||h_{g,u}||^2}{\sigma_o^2 d_{g,u}^{\alpha(\phi_{g,u})}} < x\right] = F_{||h_{g,u}||^2}\left(\frac{\sigma_o^2 d_{g,u}^{\alpha(\phi_{g,u})}x}{P_g}\right)$$
$$= \frac{1}{\Gamma(m_{g,u}N_t)}\Upsilon\left(m_{g,u}N_t, \frac{m_{g,u}\sigma_o^2 d_{g,u}^{\alpha(\phi_{g,u})}x}{\Omega_{g,u}P_g}\right). \tag{A.2}$$

Using the series representation of the lower incomplete gamma function as in [19, 8.352.1] and substituting the resulting (A.2) in (A.1) and thus performing certain substitutions and reductions, we obtain

$$\Xi_{g,u}^{\text{avg}} = 1 - \vartheta\sqrt{N_p}\sum_{l=0}^{m_{g,u}N_t-1}\frac{1}{\mathcal{A}l!}\int_{\mathcal{A}\xi_{g,u}}^{\mathcal{A}\delta_{g,u}} t^l\exp(-t)dt, \tag{A.3}$$

where $\mathcal{A} = \frac{m_{g,u}\sigma_o^2}{\Omega_{g,u}P_g}d_{g,u}^{\alpha(\phi_{g,u})}$. On evaluating the above integral, the expression in Theorem 1 can be derived.

Appendix B
Proof of Corollary 1

To derive the BLER in Corollary 1, we invoke the following series representation of lower incomplete Gamma function [15]

$$\Upsilon\left(a, \frac{x}{b}\right) = \sum_{n=0}^{M}\frac{1}{\Gamma(a+n+1)b^{a+n}}x^{a+n}\exp\left(-\frac{x}{b}\right), \tag{B.1}$$

where M equals infinity provides exact values of $\Upsilon(\cdot,\cdot)$. However, even for $M = 50$, the series converges to sufficient accuracy. After using (B.1) in (A.2) and the obtained result in (A.1), one can evaluate the resulting integral to obtain the expression in (13).

Appendix C
Proof of Corollary 2

To derive the BLER at $P_g \to \infty$, we first use the following series expansion [20]

$$\Upsilon(\alpha, x) = x^\alpha\sum_{\epsilon=0}^{\infty}\frac{(-1)^\epsilon x^\epsilon}{\epsilon!\,(\alpha+\epsilon)} \underset{x\to 0}{\simeq} \frac{x^\alpha}{\alpha}. \tag{C.1}$$

Using the above approximation in (A.2) and substituting the result in (A.1), we can express

$$\Xi_{g,u}^{\text{asy}}(\mathcal{R}_c, h) \underset{P_g\to\infty}{\simeq} \vartheta\sqrt{N_p}\int_{\xi_{g,u}}^{\delta_{g,u}}\frac{1}{\Gamma\left(m_{g,u}N_t+1\right)}$$
$$\times\left(\frac{m_{g,u}\sigma_o^2 d_{g,u}^{\alpha(\phi_{g,u})}x}{\Omega_{g,u}P_g}\right)^{m_{g,u}N_t}dx. \tag{C.2}$$

Evaluation of the above integral yields the expression in Corollary 2.

Acknowledgment

This work was supported by the Luxembourg National Research Fund (FNR)-5G-Sky Project, ref. 13713801, and the SMC funded Micro5G project.

References

[1] M. M. Azari *et al.*, "Evolution of non-terrestrial networks from 5G to 6G: A survey," *IEEE Communications Surveys Tutorials*, vol. 24, no. 4, pp. 2633–2672, 2022.

[2] M. M. Azari, S. Solanki, S. Chatzinotas, and M. Bennis, "THz-empowered UAVs in 6G: Opportunities, challenges, and trade-offs," *IEEE Commun. Mag.*, vol. 60, no. 5, pp. 24–30, 2022.

[3] G. Durisi, T. Koch, and P. Popovski, "Toward massive, ultrareliable, and low-latency wireless communication with short packets," *Proc. IEEE*, vol. 104, no. 9, pp. 1711–1726, 2016.

[4] C. Pan, H. Ren, Y. Deng, M. Elkashlan, and A. Nallanathan, "Joint blocklength and location optimization for URLLC-enabled UAV relay systems," *IEEE Commun. Lett.*, vol. 23, no. 3, pp. 498–501, 2019.

[5] H. Ren, C. Pan, K. Wang, W. Xu, M. Elkashlan, and A. Nallanathan, "Joint transmit power and placement optimization for URLLC-enabled UAV relay systems," *IEEE Trans. Veh. Technol.*, vol. 69, no. 7, pp. 8003–8007, 2020.

[6] H. Ren, C. Pan, K. Wang, Y. Deng, M. Elkashlan, and A. Nallanathan, "Achievable data rate for URLLC-enabled UAV systems with 3-D channel model," *IEEE Wireless Commun. Lett.*, vol. 8, no. 6, pp. 1587–1590, 2019.

[7] K. Wang, C. Pan, H. Ren, W. Xu, L. Zhang, and A. Nallanathan, "Packet error probability and effective throughput for ultra-reliable and low-latency UAV communications," *IEEE Trans. Commun.*, vol. 69, no. 1, pp. 73–84, 2021.

[8] P. Raut, K. Singh, W.-J. Huang, C.-P. Li, and M.-S. Alouini, "Reliability analysis of FD-enabled multi-UAV systems with short-packet communication," *IEEE Trans. Veh. Technol.*, vol. 70, no. 11, pp. 12 191–12 196, 2021.

[9] L. Yuan, N. Yang, F. Fang, and Z. Ding, "Performance analysis of UAV-assisted short-packet cooperative communications," *IEEE Trans. Veh. Technol.*, vol. 71, no. 4, pp. 4471–4476, 2022.

[10] U. Singh, S. Solanki, D. S. Gurjar, P. K. Upadhyay, and D. B. d. Costa, "Wireless power transfer in two-way af relaying with maximal-ratio combining under Nakagami-*m* fading," in *2018 14th International Wireless Communications Mobile Computing Conference (IWCMC)*, 2018, pp. 169–173.

[11] P. Yang, X. Xi, K. Guo, T. Q. S. Quek, J. Chen, and X. Cao, "Proactive UAV network slicing for URLLC and mobile broadband service multiplexing," *IEEE J. Sel. Areas Commun.*, vol. 39, no. 10, pp. 3225–3244, 2021.

[12] A. Al-Hourani, S. Kandeepan, and S. Lardner, "Optimal LAP altitude for maximum coverage," *IEEE Wireless Commun. Lett.*, vol. 3, no. 6, pp. 569–572, 2014.

[13] S. Solanki, J. Park, and I. Lee, "On the performance of IRS-aided UAV networks with NOMA," *IEEE Trans. Veh. Technol.*, vol. 71, no. 8, pp. 9038–9043, 2022.

[14] M. M. Azari, F. Rosas, K.-C. Chen, and S. Pollin, "Ultra reliable UAV communication using altitude and cooperation diversity," *IEEE Trans. Commun.*, vol. 66, no. 1, pp. 330–344, 2018.

[15] S. Solanki, S. Gautam, S. K. Sharma, and S. Chatzinotas, "Ambient backscatter assisted co-existence in aerial-IRS wireless networks," *IEEE Open Journal of the Communications Society*, vol. 3, pp. 608–621, 2022.

[16] D.-D. Tran, S. K. Sharma, S. Chatzinotas, I. Woungang, and B. Ottersten, "Short-packet communications for MIMO NOMA systems over Nakagami-*m* fading: BLER and minimum blocklength analysis," *IEEE Trans. Veh. Technol.*, vol. 70, no. 4, pp. 3583–3598, 2021.

[17] Y. Polyanskiy, H. V. Poor, and S. Verdu, "Channel coding rate in the finite blocklength regime," *IEEE Trans. Inf Theory*, vol. 56, no. 5, pp. 2307–2359, 2010.

[18] S. Boyd and L. Vandenberghe, *Convex Optimization*, Cambridge university press, 2004.

[19] I. S. Gradshteyn and I. M. Ryzhik, "Tables of integrals, series and products," 7th ed., New York, USA, Academic, 2007.

[20] S. Solanki, P. K. Sharma, and P. K. Upadhyay, "Adaptive link utilization in two-way spectrum sharing relay systems under average interference-constraints," *IEEE Syst. J.*, vol. 12, no. 4, pp. 3461–3472, 2018.